

# On the existence of patterns for a diffusion equation on a convex domain with nonlinear boundary reaction

Neus Cónsul<sup>(1)</sup> and Àngel Jorba<sup>(2)</sup>

8th July 2004

(1) Departament de Matemàtica Aplicada I, Universitat Politècnica de Catalunya, Diagonal 647, 08028 Barcelona, Spain. E-mail: [neus.consul@upc.es](mailto:neus.consul@upc.es)

(2) Departament de Matemàtica Aplicada i Anàlisi, Universitat de Barcelona, Gran Via 585, 08007 Barcelona, Spain. E-mail: [angel@maia.ub.es](mailto:angel@maia.ub.es)

## Abstract

We consider a diffusion equation on a domain  $\Omega$  with a cubic reaction at the boundary. It is known that there are no patterns when the domain  $\Omega$  is a ball, but the existence of such patterns is still unknown in the more general case in which  $\Omega$  is convex. The goal of this paper is to present numerical evidence of the existence of nonconstant stable equilibria when  $\Omega$  is the unit square. These patterns are found by continuation of families of unstable equilibria that bifurcate from constant solutions.

## 1 Introduction

In this paper we focus on the existence of nonconstant equilibrium solutions for the following diffusion equations with nonlinear reactions on the boundary,

$$\begin{cases} u_t - \Delta u = 0, & \text{in } \Omega, t > 0, \\ u_\nu = k f(u), & \text{on } \partial\Omega, t > 0, \\ u(0, x) = \psi(x) \in H^1(\Omega). \end{cases} \quad (1)$$

Here  $\Omega \subset \mathbb{R}^2$  is a bounded domain with a  $C^1$  piecewise connected boundary,  $k$  is a real positive parameter, and  $u_\nu$  denotes the outer normal derivative. The boundary nonlinearity is given by a cubic reaction  $f(u) = -u(u - a)(u - b)$ ,  $a < 0 < b$ .

There are many problems in chemistry (heterogeneous catalysis), biology (population dynamics) and engineering (heat transfer) for instance, modelled by this kind of equations (see [Gri96, MO84]). An important issue is the nonlinearity in the boundary reaction. This nonlinear condition results in a more complex model than the usual linear approximations but it allows for a better modelling of the boundary phenomena. The evolution of the

solutions of (1) is determined by the different equilibria (stable and unstable) and their connections through stable and unstable manifolds.

It is well known that for fixed  $k > 0$ , problem (1) generates a well defined nonlinear semigroup in  $H^1(\Omega)$ , the solutions enter  $W^{1,p}(\Omega)$  for any  $1 < p < \infty$  and are classical for  $t$  positive. Moreover, the flow has an attractor  $\mathcal{A}_k$  which is a compact invariant set that attracts each bounded set of  $H^1(\Omega)$  (see [ACRB00]). This attractor contains all the equilibria of the problem and it must be connected, but the shape or the possible connections between them is a very complicated question (see [Hal88]).

Following the approach of H. Amann [Ama88], this problem admits a semilinear formulation, that is, it can be written in the form

$$u_t = Au + kF(u). \quad (2)$$

Here  $A$  is the linear part and it is defined as  $A(u)v = \int_{\Omega} (\nabla u \nabla v - uv) dx$ . The nonlinear functional  $F(u) = u + \gamma' f(\gamma u)$ , where  $\gamma$  and  $\gamma'$  denote the trace operator on the boundary and the dual of the trace operator on the boundary, respectively. As it is usual the stability of an equilibrium solution of (2),  $u_0$ , can be determined by linearization, that is, by computing the spectrum  $\sigma(L)$  of the linear operator  $L = A + kDF(u_0)$ . In this case, the spectrum consists only of eigenvalues and all of them are real (see [Cón96]). So, if  $\sigma(L) \subset \{\text{Re}\lambda > 0\}$  we have that  $u_0$  is asymptotically stable, if there is a negative eigenvalue  $u_0$  is unstable and, if zero is the first eigenvalue  $u_0$  can be either stable or unstable.

The solutions of the stationary problem

$$\begin{cases} -\Delta u = 0, & \text{in } \Omega, \\ u_{\nu} = kf(u), & \text{on } \partial\Omega. \end{cases}$$

are equilibrium solutions for (1). The only constant equilibria correspond to the zeroes of  $f$ ,  $u = a$ ,  $u = 0$  and  $u = b$ . The Lyapunov stability of these equilibria can be established, as we mentioned before, by looking at the spectrum of a suitable linear operator. In this way the equilibria  $u = a$  and  $u = b$  are asymptotically stable while  $u = 0$  is unstable.

The nonconstant stable equilibrium solutions, often so called patterns, are of relevant importance. They are related with morphogenesis phenomena. We are concerned by the existence of nonconstant stable equilibrium solutions of (1) depending on the geometry of the domain  $\Omega$ , which is going to be connected in all the paper. If the domain  $\Omega$  were disconnected we could construct trivial patterns assigning two different (stable) constants in each component of the domain. There are some results in the literature related to the existence and nonexistence of patterns for (1). If  $\Omega$  is a ball in  $\mathbb{R}^n$ ,  $n \geq 2$ , it is known that there are no patterns for problem (1) for any  $k > 0$ , that is, only constant solutions can be stable equilibria, see [Cón96]. On the other hand, the formation of patterns can be achieved with a typical cubic nonlinearity when the domain loses its convexity. This is the case of the so called dumbbell domains, which consist of two disjoint domains joined by a thin and/or short channel, see [CSM99]. Patterns also appear when the boundary of the domain  $\Omega$  is disconnected, like a domain with holes, see [Cón96].

A very well known problem is

$$\begin{cases} u_t - \Delta u = kf(u), & \text{in } \Omega, t > 0, \\ u_\nu = 0, & \text{on } \partial\Omega, t > 0, \\ u(0, x) = \psi(x) \in H^1(\Omega), \end{cases} \quad (3)$$

where the reaction occurs in the interior of the domain but which has some very close relations with (1). For this problem Casten and Holland in [CH78] and, independently, Matano in [Mat79] show the nonexistence of patterns when  $\Omega$  is a convex domain.

For nonlinear boundary reactions like (1) it is known, as said before, that there are no patterns when the domain  $\Omega$  is a ball. It is remarkable that the existence or nonexistence of such patterns is still an open question in the more general case in which  $\Omega$  is convex.

The goal of this paper is to present numerical evidence of the existence of nonconstant stable equilibria for (1),  $\Omega$  the unit square and  $f(u) = u(1 - u^2)$ . More concretely, we show that these patterns seem to exist for  $k > 2.84083164$ . This implies that the results about nonexistence of patterns in convex domains for (3) does not hold for nonlinear boundary reactions.

In [CC] X. Cabré and N. Cónsul are completing an analytical proof of an existence of patterns in convex domains, for  $k$  large enough. These analytical results give the existence of patterns for  $k$  sufficiently large and the location of jumps on the boundary for  $k \rightarrow \infty$ , depending on the considered domain  $\Omega$ . Here we give numerical evidence of the existence of such patterns and, in add, we study their stability as  $k$  decreases.

Our search of stable equilibria proceeds in a systematic way, by following families of nonconstant equilibrium solutions. More concretely, we first compute the families of equilibria that bifurcate from the unstable solution  $u = 0$ , for the range  $0 < k < 3$ , and then we follow the branched families up to  $k = 10$ . All these families are unstable for values of  $k$  close to the bifurcation but, when  $k$  grows, one of them undergoes a new bifurcation and becomes stable. It seems that these stable solutions persist when  $k$  goes to infinity (see [CC]).

The paper is organized as follows. Section 2 contains the study (analytical and numerical) of the critical values of  $k$  for which there are equilibrium solutions branching off from the origin. Section 3 discusses the results of a numerical computation of these branches, including their stability. Finally, in Section 4, we have included a short description of the numerical tools used in the study.

## 2 Linearization around $u = 0$

We want to study families of nonconstant equilibrium solutions of (1), depending on the parameter  $k$ . More concretely, we will look for families branching off from the constant equilibria. As we mentioned in the introduction, by the linear principle of stability, we know that the constant solutions  $u = -1$  and  $u = 1$  are both asymptotically stable for all  $k$  and, therefore, nothing can bifurcate from them. In [Cón96] it is proved that, for  $k$  sufficiently small, all the equilibrium solutions are constant and, therefore, they must coincide with the zeroes of  $f$ . In this context, it is natural to look for nonconstant

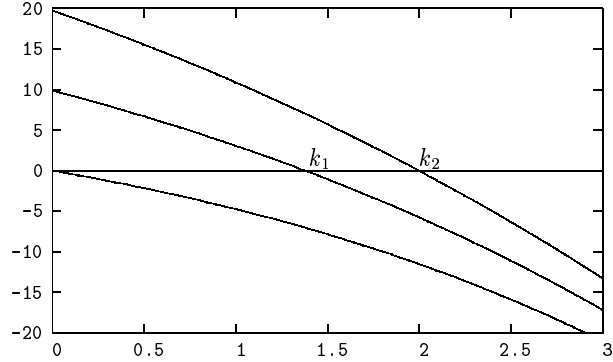


Figure 1: Continuation of the first three eigenvalues of the linearization of (1) around  $u = 0$  w.r.t.  $k$  ( $k$  is shown in the horizontal axis).

equilibrium solutions as bifurcations of the unstable solution  $u = 0$ . Hence, the first step must be to compute the spectrum of the linearization of the equation at  $u = 0$  to detect eigenvalues that cross 0.

We have discretized the operator  $L$  at  $u = 0$  using linear finite elements (see Section 4). We have computed the first three eigenvalues for  $k \in [0, 3]$ , and we have represented them in Figure 1. Let us observe that these eigenvalues decrease as  $k$  increases. They go from the eigenvalues of the Laplacian with Neumann condition ( $k = 0$ ) to the eigenvalues of the Steklov problem (see [Ban80]),

$$\begin{cases} \Delta u = 0 & \text{in } \Omega, \\ u_\nu = k u, & \text{on } \partial\Omega. \end{cases} \quad (4)$$

The eigenvalues of (4) coincide with the values of  $k$  for which  $L$  has a zero eigenvalue and, therefore, the spectrum of (4) gives the values of  $k$  for which we can expect a bifurcation from  $u = 0$ . Moreover, for each eigenvalue  $k$  of (4), the eigenspace also coincides with the kernel of  $L - kI$ .

Note that, for  $k = 0$ , (1) is an homogeneous Neumann problem and it is well known that its spectrum consists only of the real nonnegative eigenvalues  $\lambda_{m,n} = (m^2 + n^2) \pi^2$ ,  $m, n \in \mathbb{N}$ . They are simple when  $n = m$ , and of multiplicity two otherwise. Note that, for this homogeneous problem, any constant is a solution.

For  $k > 0$ , the first eigenvalue  $\lambda_0(k)$  is always negative, the second and third eigenvalues  $\lambda_{1,2}(k)$  cross zero at  $k = k_{1,2}$  respectively, as it is shown in Figure 1. We have computed the values  $k_{1,2}$  from the finite element discretization, using three meshes (of 8321, 33025 and 131585 nodes) and two steps of extrapolation to obtain the values  $k_1 \approx 1.37650548469797$  and  $k_2 \approx 2.00000000015288$ .

As this computation does not assume any kind of special form for the eigenfunctions, we can also use it to estimate the geometric dimension of the eigenvalues. It turns out that this dimension is 2 for  $k = k_1$  and 1 for  $k = k_2$ .

As  $\Omega = [0, 1] \times [0, 1]$ , we can compute analytically the eigenvalues and eigenfunctions of the Steklov problem by separating the variables and, therefore, we can use them to test the accuracy of our finite element computation. The eigenvalues are  $k = 2$  and

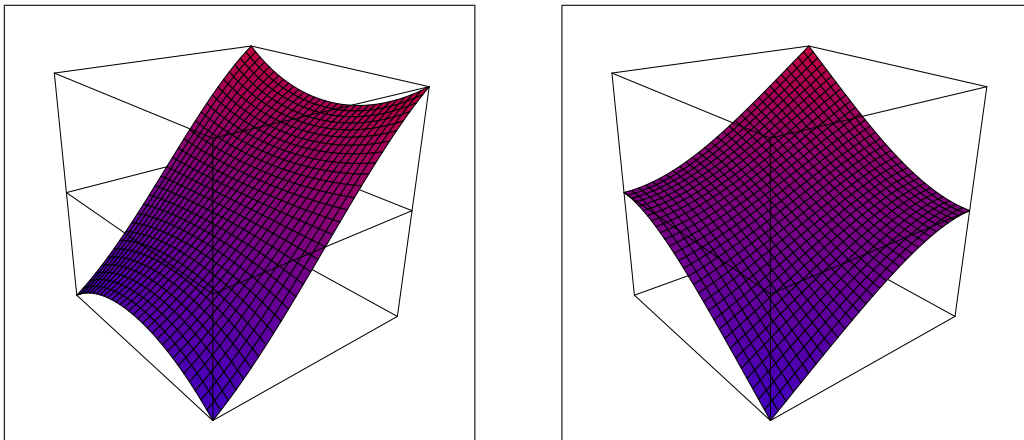


Figure 2: Eigenfunctions of the Steklov problem for  $k = k_1$ . Horizontal plane:  $(x, y)$  coordinates. Vertical axis: value of  $u$ . The colour goes from blue for  $u = -1$  to red for  $u = 1$ . The intersection between the plane  $u = 0$  and the box containing the figures is marked with a square.

$k = 2\omega \tanh \omega$ , where  $\omega$  are the zeros of the equations  $\tanh \omega = \coth \omega$  or  $\tanh \omega = \tan \omega$ . The eigenfunctions are  $u(x, y) = (1 - 2x)(1 - 2y)$  for the eigenvalue 2, and  $u(x, y) = (e^{2\omega x} + e^{2\omega(1-x)}) (\cos(2\omega y) - \tanh \omega \sin(2\omega y))$  (and the ones obtained by changing  $x$  and  $y$ ) in the other cases. Note that there are two eigenfunctions for each eigenvalue, except for  $k = 0$  and  $k = 2$ , that has only one. As the eigenfunctions for  $k > 0$  have been obtained by separating the variables, we can only ensure that the geometric multiplicity of the eigenvalues is at least 2 for  $k \neq 2$ , and at least 1 for  $k = 2$ . The geometric multiplicity of  $k = 0$  is already known to be 1.

In what follows we will focus on the first three eigenvalues. For definiteness, we will denote them as  $k_0 = 0$ ,  $k_1 = 1.376505484672535$  and  $k_2 = 2$ .

The agreement between the analytical and numerical results is quite good. Referring the multiplicities of the eigenvalues it seems that the only eigenfunctions are the ones obtained analytically by separating the variables in the Steklov problem. Note that the multiplicities coincide with those of the corresponding eigenvalues (see Figure 1) for  $k = 0$ .

### 3 Bifurcating branches

In this section we will make use of some properties of the equilibria of (1). Due to the particular form of the domain and the equation, note that if  $u$  is a solution of (1), any rotation  $\frac{\pi}{2}$  of  $u$  also satisfies (1). Moreover, due to the parity properties of  $f$ , if  $u$  is a solution,  $-u$  is also a solution. Finally, from the maximum principle of Hopf it follows that all solutions are bounded by  $-1 \leq u \leq 1$  (see [Cón96]).

Next, we will discuss the first two bifurcations, corresponding to the values  $k = k_{1,2}$ . As we will see, this is enough to find stable nonconstant equilibria, which is the main goal of this paper.

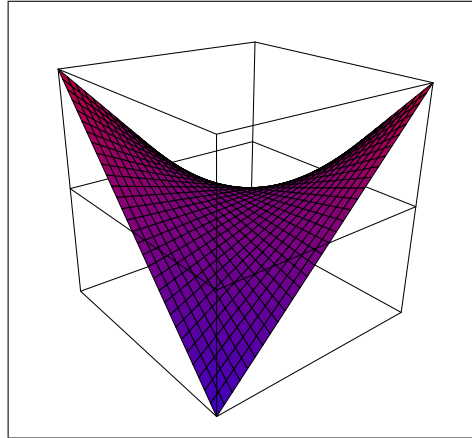


Figure 3: Eigenfunctions of the Steklov problem for  $k = k_2$ . The axis are as in Figure 2.

### 3.1 First bifurcation

It corresponds to  $k = k_1$ . We recall that, in this case, there exist two linearly independent eigenfunctions (shown in Figure 2) with eigenvalue zero. A numerical study (see Section 4) shows that this bifurcation does not give rise to a bifurcating two dimensional manifold but only to 4 curves that are defined for  $k > k_1$ . In fact, we have computed these curves for  $k \in (k_1, 10]$ . We will see in a moment that we can use the symmetries of the problem to reduce these 4 curves to only 2.

The first branch consists of solutions  $u(x_1, x_2)$  such that  $u(\frac{1}{2}, x_2) = 0$  for all  $x_2 \in [0, 1]$ ,  $u(x_1, x_2) < 0$  if  $x_1 < \frac{1}{2}$  and  $u(x_1, x_2) > 0$  if  $x_1 > \frac{1}{2}$ . When  $k$  increases, the “left half part” of the solution tends to  $-1$  and the “right half part” tends to  $1$  on the boundary. The other side of this branch corresponds to change the sign of the solutions. Apparently, when  $k \rightarrow \infty$  the solution becomes an harmonic function which is piecewise constant on the boundary, jumping from  $-1$  to  $1$  or from  $1$  to  $-1$  at  $(x_1, x_2) = (\frac{1}{2}, 0)$  or  $(\frac{1}{2}, 1)$ , as it is shown in [CC]. Applying the  $\frac{\pi}{2}$ -rotational symmetry mentioned before we obtain a new bifurcating branch.

The second bifurcating branch consists of solutions  $u(x_1, x_2)$  such that  $u(x_1, x_2) = 0$  for  $x_1 = x_2$ ,  $u(x_1, x_2) < 0$  if  $x_1 > x_2$  and  $u(x_1, x_2) > 0$  if  $x_1 < x_2$ . When  $k$  increases the positive part goes to  $1$  and the negative part goes to  $-1$  on the boundary. As before, the other side of this branch corresponds to change the sign of the solutions and, the  $\frac{\pi}{2}$ -rotational symmetry gives a new bifurcating branch.

Near the bifurcation point  $k = k_1$ ,  $u = 0$ , all the equilibrium solutions are unstable due to the instability of  $u = 0$  and the continuity of the spectrum.

A computation of the eigenvalues of the solutions along the branches shows that the first branch ((1a) in Figure 6) is unstable and changes its stability at  $k = k_1^s \approx 2.84083164$  becoming stable (the critical equilibrium for  $k = k_1^s$  is shown in Figure 5, left) but that the second branch ((1b) in Figure 6) is always unstable. In Figure 4 we display the first eigenvalue of the branch (1a) from  $k = k_1$  to  $k = 4$ . As far as we know, this computation is the first evidence of the existence of nonconstant stable equilibria for a convex domain. We have followed this stable branch up to  $k = 10$  and it looks persistent when  $k$  increases.

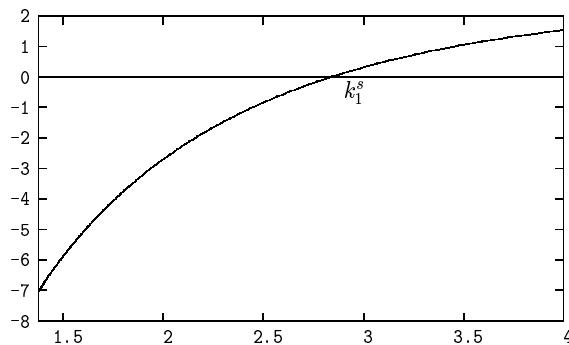


Figure 4: Continuation of the first eigenvalue along the branch (1a). The value of  $k$ ,  $k_1 \leq k \leq 4$ , is shown in the horizontal axis.

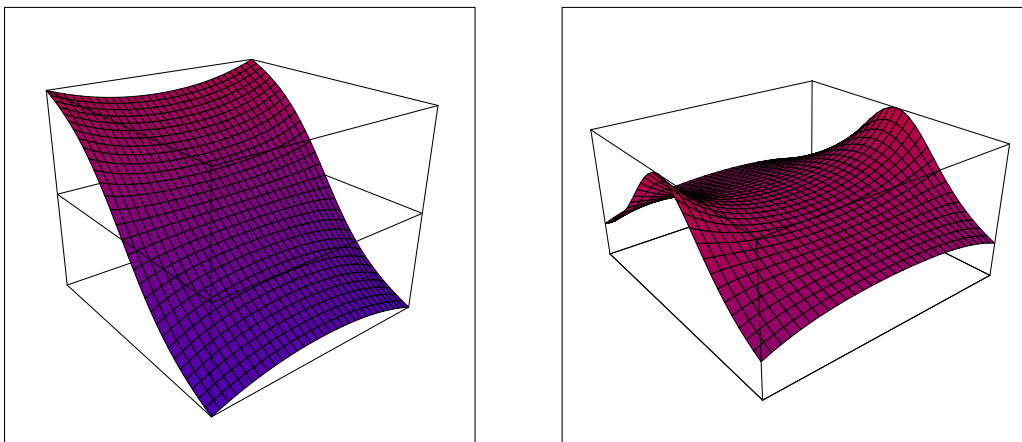


Figure 5: Change of stability on the branch (1a). Left: Critical equilibrium at  $k = k_1^s$ . Right: Kernel of the linearization around this equilibrium;  $u = 0$  corresponds to the lower side of the box. The colour goes from blue for  $u = -1$  to red for  $u = 1$ . The mesh used in the drawings is not the mesh used for the computations.

The persistence for  $k \rightarrow \infty$  agrees with some recent analytical results (see [CC]).

Let us focus on the change of stability of the branch (1a). The computation of the spectrum shows that the kernel of the linearized operator has dimension 1 (see Figure 5, right) so that we expect a one-dimensional bifurcating manifold. Our computations give a curve of equilibria that bifurcates from this point,  $k = k_1^s$ ,  $u = u_{k_1^s}$ , and is defined for  $k > k_1^s$ . When  $k$  increases, the transition curve  $u(x_1, x_2) = 0$  of the bifurcated branch moves (from  $x_1 = \frac{1}{2}$ ) to the left. As before, the opposite branch can be obtained changing the sign of the equilibrium solutions of the previous branch.

In Figure 6 we show schematically these bifurcating branches. In Figure 7 we display the equilibrium solutions corresponding to  $k = 4$  for each one of the first three branches that appear in the bifurcation scheme. The maximum and the minimum values for each solution are the following:  $u = -0.912$  and  $u = 0.912$  for (1a),  $u = -0.934$  and  $u = 0.934$  for (1b), and  $u = -0.961$  and  $u = 0.669$  for (1c).

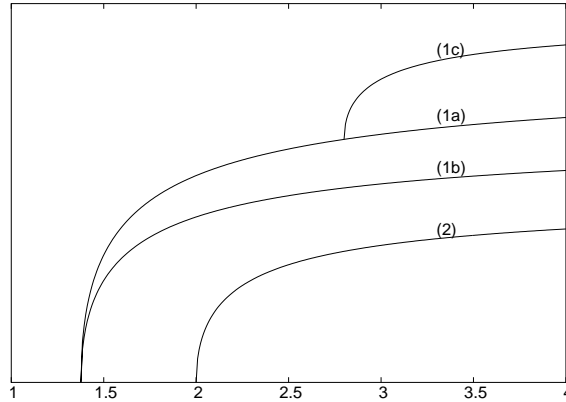


Figure 6: Schematic representation of the branches that bifurcate from the origin. The value of  $k$  is shown in the horizontal axis.

### 3.2 Second bifurcation

This bifurcation corresponds to  $k = k_2$ . We recall that, in this case, the eigenspace has dimension one (see Figure 3) so that we only expect a single bifurcating curve.

One of the branches consists of solutions  $u(x_1, x_2)$  such that  $u(x_1, \frac{1}{2}) = u(\frac{1}{2}, x_2) = 0$ ,  $u(x_1, x_2) < 0$  if  $(x_1, x_2) \in [0, \frac{1}{2}]^2 \cup [\frac{1}{2}, 1]^2$  and positive otherwise. The other side of the bifurcating curve is obtained by simply changing the sign of the solutions. Note that, for these kind of equilibria, changing the sign is equivalent to a  $\frac{\pi}{2}$ -rotation. The computation of the dominant eigenvalues of the linearization of the equation at these equilibria shows that they are unstable in the computed range  $k_2 < k \leq 10$ .

This branch is also shown, schematically, in Figure 6 labelled as (2). In Figure 7 we show the equilibrium solution corresponding to  $k = 4$  for the fourth branch (2) in Figure 6. In this case the maximum and the minimum values are  $u = -0.847$  and  $u = 0.847$ .

## 4 Numerical methods

The variational formulation of (1) is

$$\langle u_t, v \rangle + a(u, v) = k \langle f(u), v \rangle_{\partial\Omega},$$

for any  $v$  in the space of test functions  $V$ . Here,  $\langle \cdot, \cdot \rangle$  and  $\langle \cdot, \cdot \rangle_{\partial\Omega}$  denote the scalar products in  $L^2(\Omega)$  and  $L^2(\partial\Omega)$ , respectively and

$$a(u, v) = \int_{\Omega} \nabla u \cdot \nabla v \, dx.$$

We will use the standard finite element formulation, based on linear triangular elements. Therefore, we have a linear space of piecewise linear polynomials, of dimension  $N$  and using the usual approximation in this space and the Galerkin method, we obtain a set of nonlinear ordinary differential equations for the  $N$  coefficients  $u_i$ ,  $1 \leq i \leq N$ , of



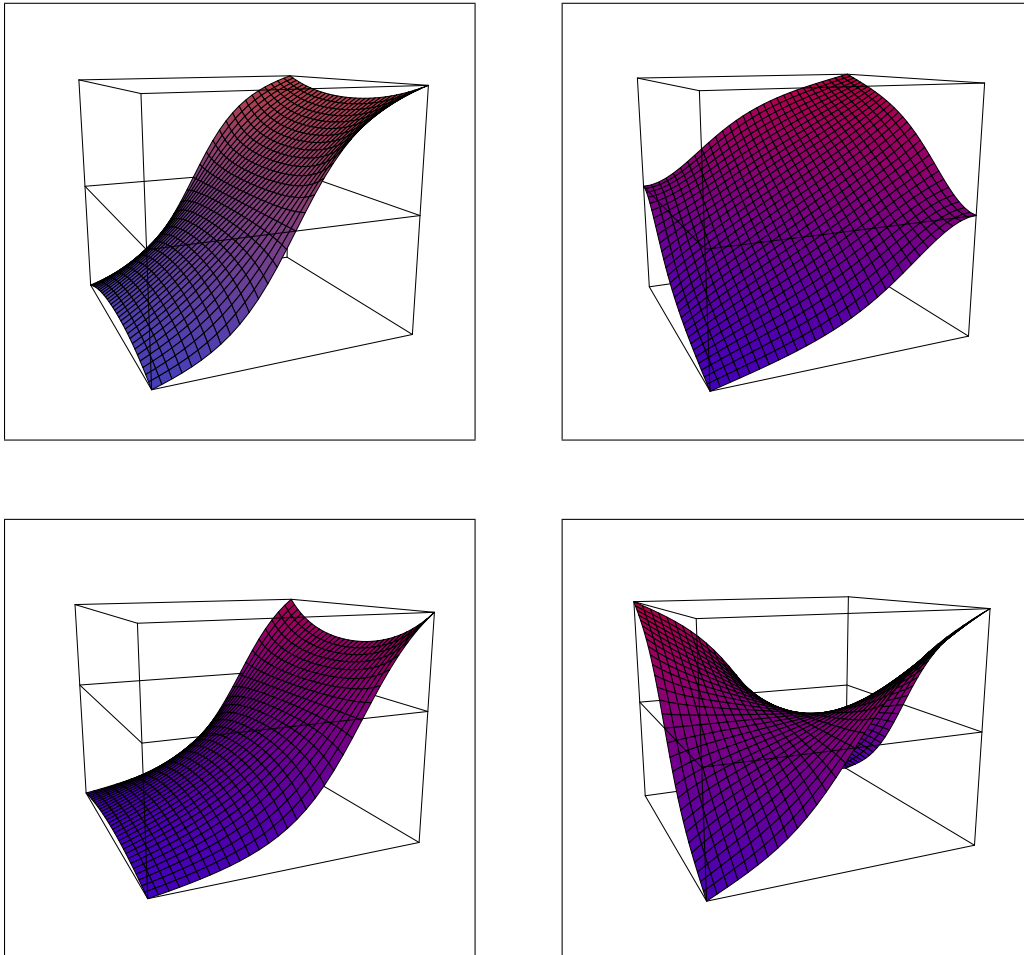


Figure 7: Equilibria, for  $k = 4$ , of branch (1a) (upper left), (1b) (upper right), (1c) (bottom left) and (2) (bottom right). The axis are as in Figure 2.

the approximations of  $u$ . The system can be expressed in the matrix form,

$$A\dot{u} + Bu = kF(u), \tag{5}$$

with  $u = (u_1, \dots, u_N)^T$  and

$$\begin{aligned} A &= (\langle \varphi_i, \varphi_j \rangle)_{i,j}, \\ B &= (a(\varphi_i, \varphi_j))_{i,j}, \\ F(u) &= \left( \left\langle f \left( \sum_{i=1}^N u_i \varphi_i \right), \varphi_j \right\rangle_{\partial\Omega} \right)_j, \end{aligned}$$

where  $1 \leq i, j \leq N$ , and  $\{\varphi_i\}_{1 \leq i \leq N}$  is the usual basis in the space of  $N$ -piecewise linear polynomials.

Let us observe that this variational formulation coincides with de semilinear formulation (2) of the continuous problem.

## 4.1 Equilibria

The equilibrium solutions of (5) satisfy

$$Bu - kF(u) = 0. \quad (6)$$

Our numerical method is based on solving this equation by means of the Newton method. The advantage of this approach is that the equilibria are found regardless of their stability.

The continuation procedure is very standard; it is based on including the parameter  $k$  as an ordinary unknown. To summarize how it works, assume that  $p_*^{(0)} = (u_*^{(0)}, k_*^{(0)})$  is an approximation to an equilibrium. Then, the Newton method requires to solve a linear system with an extra unknown ( $k$ ). This implies that, generically, we have a 1-D affine space of solutions. Among them, we select the one of minimum  $L^2$ -norm; this implies that we are looking for the point on the manifold (in the  $(u, k)$  space) of solutions closest to the initial condition. Once the Newton method has converged to a point  $p^{(0)} = (u^{(0)}, k^{(0)})$ , the kernel of the linearization at  $p^{(0)}$  of the operator  $(u, k) \mapsto Bu - kF(u)$  gives the unitary tangent vector  $\tau^{(0)}$  to the curve of solutions at this point. Then, we can predict an approximation  $p_*^{(1)} = p^{(0)} + h\tau^{(0)}$  to a new point of the curve. If the value of  $h$  is too large, the Newton method starting at  $p_*^{(1)}$  will not converge to a point on the curve, and if it is too small we will need to compute a lot of points to advance a fixed distance on the curve. The adjustment of the value of  $h$  is done automatically: if the Newton method needs more than 3 iterates to converge,  $h$  is halved; if it needs only 1, it is doubled.

## 4.2 Stability

The stability is found by rewriting (5) as

$$\dot{u} = A^{-1}(-Bu + kF(u)).$$

If  $u_0$  is a solution of (6), the linearization around  $u_0$  is given by the operator  $L : H^1 \rightarrow H^1$ ,

$$Lv = A^{-1}(-B + kDF(u_0))v.$$

Note that this coincides with the discretization of the linearization of (2). As the spectrum of  $L$  only consists of real eigenvalues (see [Cón96]), we look for couples  $(\lambda, v) \in \mathbb{R} \times H^1$  such that

$$(-B + kDF(u_0))v = \lambda Av.$$

The equilibrium  $u_0$  is asymptotically stable iff the first eigenvalue is strictly positive. The dominant part of the spectra (including the eigenvalues) has been obtained by means of an inverse power method with a suitable shift.

## 4.3 Bifurcation analysis

The bifurcation of  $u = 0$  for  $k = k_1$  corresponds to a double eigenvalue, for which the corresponding eigenspace is also of dimension 2. To study the neighbourhood of this singular point, we have computed two linearly independent eigenfunctions  $v_1$  and  $v_2$ , and

we have considered the “circle” of values  $v_1 \cos \theta + v_2 \sin \theta$  for  $\theta \in \mathbb{S}^1$  as initial conditions for a Newton method (we recall that  $k$  is also an unknown, see Section 4.1). We have used these initial conditions for a mesh of 1000 equispaced values of  $\theta$ , and we have only found 8 branches going out from the singular point (in other words, we have only found 4 curves going through the bifurcation point). If we take into account the symmetries of the problem, the 8 branches can be reduced to 2. The eigenfunctions tangent to these branches are the ones shown in Figure 2.

The bifurcation of  $u = 0$  for  $k = 2$  and the bifurcation on the branch (1c), in Figure 6, for  $k = 2.84083164$  correspond to a single null eigenvalue, whose eigenspace is also of dimension 1. Therefore, in both cases we have obtained the corresponding eigenfunction  $v$  and we have used the values  $u \pm hv$ , for  $h$  small, as initial values for the Newton method. As before, the initial value for  $k$  is the value at the bifurcation point, but the Newton method handles  $k$  as a variable.

#### 4.4 Error estimation

The error estimation is based on comparing the solutions with the results corresponding to a finer mesh, obtained by halving all the triangles of the initial triangulation. The comparison is used as an error estimate on each node, and it is used to refine the mesh around the nodes with a too large error estimate. For the computation of Delaunay triangulations we have used the library Triangle [She], which has proven to be excellent. The remaining programs have been coded in C by the authors, taking advantage of the particularities of the problem.

During the continuation process (see Figure 6), we have always used the same mesh. The error estimation shows that the error grows when  $k$  becomes larger. This is expected since the transition in these equilibria is faster when  $k$  increases. The mesh we have used for the continuation produces an error estimate around  $10^{-4}$  for  $k = 4$ .

## Acknowledgements

The authors thank X. Cabré and J. Solà-Morales for interesting discussions and remarks. N. Cónsul acknowledges support from MCyT grant BFM 2002-04613-C03-01. À. Jorba has been supported by the MCyT/FEDER grant BFM2003-07521-C02-01, the Catalan CIRIT grant 2001SGR-70 and DURSI.

## References

- [ACRB00] J.M. Arrieta, A.N. Carvalho, and A. Rodríguez-Bernal. Attractors of parabolic problems with nonlinear boundary conditions. Uniform bounds. *Comm. Partial Differential Equations*, 25(1-2):1–37, 2000.
- [Ama88] H. Amann. Parabolic evolution equations and nonlinear boundary conditions. *J. Differential Equations*, 72(2):201–269, 1988.

- [Ban80] C. Bandle. *Isoperimetric inequalities and applications*, volume 7 of *Monographs and Studies in Mathematics*. Pitman (Advanced Publishing Program), Boston, Mass., 1980.
- [CC] X. Cabré and N. Cónsul. Minimizers for boundary reactions: renormalized energy, locations of singularities, and applications. Work in progress.
- [CH78] R.G. Casten and C.J. Holland. Instability results for reaction diffusion equations with Neumann boundary conditions. *J. Differential Equations*, 27(2):266–273, 1978.
- [Cón96] N. Cónsul. On equilibrium solutions of diffusion equations with nonlinear boundary conditions. *Z. Angew. Math. Phys.*, 47(2):194–209, 1996.
- [CSM99] N. Cónsul and J. Solà-Morales. Stability of local minima and stable nonconstant equilibria. *J. Differential Equations*, 157(1):61–81, 1999.
- [Gri96] P. Grindrod. *The theory and applications of reaction-diffusion equations*. Oxford Applied Mathematics and Computing Science Series. The Clarendon Press Oxford University Press, New York, second edition, 1996. Patterns and waves.
- [Hal88] J.K. Hale. *Asymptotic behavior of dissipative systems*, volume 25 of *Mathematical Surveys and Monographs*. American Mathematical Society, Providence, RI, 1988.
- [Mat79] H. Matano. Asymptotic behavior and stability of solutions of semilinear diffusion equations. *Publ. Res. Inst. Math. Sci.*, 15(2):401–454, 1979.
- [MO84] J.D. Murray and G.F. Oster. Generation of biological pattern and form. *IMA J. Math. Appl. Med. Biol.*, 1(1):51–75, 1984.
- [She] J.R. Shewchuk. <http://www-2.cs.cmu.edu/~quake/triangle.html>.